Advances in Materials Research, *Vol. 6, No. 1 (2017) 27-43*
DOI: https://doi.org/10.12989/amr.2017.6.1.027

Transient thermo-mechanical response of a functionally graded beam under the effect of a moving heat source

Naser S. Al-Huniti* and Sami T. Alahmad

Department of Mechanical Engineering, The University of Jordan, 11942, Amman, Jordan

(Received January 11, 2017, Revised March 7, 2017, Accepted March 8, 2017)

Abstract. The transient thermo-mechanical behavior of a simply-supported beam made of a functionally graded material (FGM) under the effect of a moving heat source is investigated. The FGM consists of a ceramic part (on the top), which is the hot side of the beam as the heat source motion takes place along this side, and a metal part (in the bottom), which is considered the cold side. Grading is in the transverse direction, with the properties being temperature-dependent. The main steps of the thermo-elastic modeling included deriving the partial differential equations for the temperatures and deflections in time and space, transforming them into ordinary differential equations using Laplace transformation, and finally using the inverse Laplace transformation to find the solutions. The effects of different parameters on the thermo-mechanical behavior of the beam are investigated, such as the convection coefficient and the heat source intensity and speed. The results show that temperatures, and hence the deflections and stresses increase with less heat convection from the beam surface, higher heat source intensity and low speeds.

Keywords: transient; thermo-mechanical; FGM; beam; moving heat source

1. Introduction

Functionally Graded Materials (FGMs) are a class of composite materials with continuous variation of material properties from one surface to another. The FGM usually consists of a ceramic part and a metal part. The resulting composite material will have the advantages of both materials, where the ceramic part has the thermal resistance ability and the metal part can support the composite with its elasticity. The importance of FGMs comes mainly from their ability to withstand severe temperature gradients. The continuous variation in the microstructure of FGMs distinguishes them from the traditional fiber-reinforced laminated composite materials, where the variation of mechanical properties is not continuous across the interface, which may result in de-bonding of layers at elevated temperatures. The use of FGMs eliminates this problem, which makes them good candidates to replace fiber-reinforced laminated composite materials in applications that involve high temperature gradients.

A heat source moving along a beam is a case that models some practical situations in different engineering applications, such as welding, grinding, metal cutting, firing a bullet in a gun barrel,

*Corresponding author, Professor, E-mail: alhuniti@ju.edu.jo

Copyright © 2017 Techno-Press, Ltd.
http://www.techno-press.org/?journal=amr&subpage=7 ISSN: 2234-0912 (Print), 2234-179X (Online)

flame or laser hardening of metals, and others. This case of loading results in transient variations in temperatures, deformations and stresses, which may result in the deterioration of the beam if the temperature gradients are severe.

The history of FGM goes back to 1972 (Lee 2013). Since then, many researchers have investigated different aspects and applications of FGM structures under mechanical and thermal load. The literature reveals a continued interest among the research community to develop efficient mathematical models to predict the static and dynamic response of structures, made of FGM (Freund 1993, Koizumi 1997, Sankar 2001, Sankar and Tzeng 2002, Zhu and Sankar 2004, Ding *et al.* 2007, Kadoli *et al.* 2008, Simsek 2010, Wang and Pan 2011, Malekzadeh and Heydarpour 2012, Zenkour and Abouelregal 2014, Malekzadeh and Shojaee 2014, Zamanzadeh *et al.* 2014, Akbaş 2015, Ebrahimi *et al.* 2016, Daouadji and Adim 2016, Jooybar *et al.* 2016a, Jooybar *et al.* 2016b).

Some investigations have considered the case of a moving heat source on homogeneous and composite materials such as (Al-Huniti *et al*. 2001) where they investigated the thermally induced displacements and stresses of a homogeneous rod under the action of a moving heat source. Al-Huniti (2004) investigated the dynamic response of a laminated beam under a moving heat source based on the classical beam theory. The beam considered was made of metallic layers with constant mechanical and thermal properties. Al-Huniti *et al*. (2004) investigated the transient variations of thermal stresses of a plate as a result of a moving heat source during welding process. Some studies appeared in the literature that deal with the case of FGM with a moving heat sources. Malekzadeh and Heydarpour (2012) determined the response of functionally graded cylindrical shells under moving thermo-mechanical loads. Malekzadeh and Shojaee (2013) investigated the dynamic response of functionally graded plates under moving heat source. Malekzadeh and Shojaee (2014) studied the thermal and dynamic response of FG beams under a moving heat source using the FEM in conjunction with Newmark's time integration scheme. Zamanzadeh *et al.* (2014) investigated the thermally-induced vibration of FG cantilever micro-beam subjected to a moving laser beam via simulating the equivalent third-order dynamic system. Malekzadeh and Monajjemzadeh (2016) studied the dynamic response of functionally graded beams in a thermal environment under a moving load.

The present work is concerned with the investigation of the transient thermo-mechanical behavior, mainly in the form of the induced temperatures, stresses and deflection, of a simply supported beam made of a functionally graded material under the action of a moving heat source. Analytical techniques are used to develop and solve the dynamic thermo-mechanical model of the beam and calculate the resulting transient temperatures, stresses and deflection as functions of time and space. In the analytical approach, the Fourier heat conduction model is used to derive the heat equation and determine the thermal history of the beam. This is then combined with the principles of dynamics, solid mechanics and beam theories to derive the governing equations of motion of the beam that is solved to determine the variations in the stresses and deflections. Transverse and axial deflections are both calculated and presented. The effects of the material grading and properties, beam geometry, heat source nature and speed are studied.

2. Modeling

2.1 Thermal model and temperature distribution

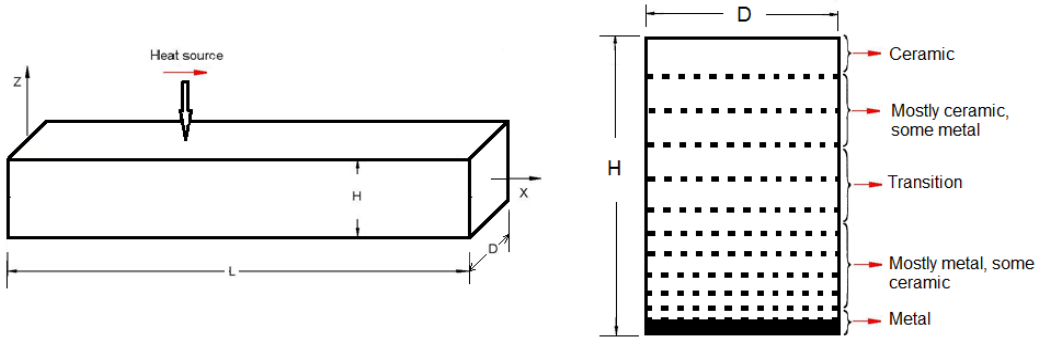

Fig. 1 The simply supported FG beam under the effect of moving heat source

A rectangular simply-supported beam of uniform thickness H and depth D, subjected to a moving heat source with constant intensity and speed is shown in Fig. 1. Initially, the beam is maintained at a uniform temperature, which is equal to the ambient temperature T_∞, then the heat source is applied on the beam starting from one end (x=0) of the beam to the other end (x=L), moving on the top surface.

The beam is made of a functionally graded material (FGM) consisting of a metal part (bottom) and ceramic part (top). Grading is in the transverse direction (z-axis), as shown in Fig. 1. Therefore, the thermal and mechanical properties of the FGM vary in the z-direction of the beam. The smooth transition of the properties in the FGM from metallic to ceramic, as shown in Fig. 1, provides thermal protection as well as structural integrity, reducing the possibilities of failure within the beam. The material properties in the axial direction are the same. In the analysis to follow, the beam is considered to be laminated, i.e., composed of thin layers in the transverse direction, in order to properly model the variation of FGM properties in that direction.

The temperature distribution in the axial direction of the beam depends on different factors such as the heat source intensity and velocity, convection coefficient, beam dimensions and thermal properties. The governing heat equation is given by

$$\rho c \frac{\partial T}{\partial t} = -\frac{\partial q}{\partial x} - \frac{hp}{DH}(T - T_\infty) + g \tag{1}$$

Where the heat flux (q) is given by Fourier's law of heat conduction

$$q = -k \frac{\partial T}{\partial x} \tag{2}$$

Elimination of q between Eqs. (1) and (2) yields

$$\rho c \frac{\partial T}{\partial t} + \frac{hp}{DH}(T - T_\infty) = g + k \frac{\partial^2 T}{\partial x^2} \tag{3}$$

In the above equations, ρ is the mass density, c is the specific heat, h is the convection coefficient, p is the perimeter of the beam, k is the thermal conductivity, $hp/DH(T-T_\infty)$ represents the convection losses from circumferential surface area of the beam, and g represents a moving plane heat source of constant strength releasing its energy continuously while moving along the x-axis with a constant speed υ. Note that Eq. (3) represents the temperature variation along the axial direction of the beam with time, i.e., $T(x,t)$.

The first step to find the temperature distribution of the FGM beam is to apply Eq. (1) in the top thin layer of the beam so the temperature distribution of that layer is found. This layer of the beam is considered very thin with homogenous properties in both the axial and the transverse directions. The temperature distribution of this layer will then be used to find that of the next layer, using the forthcoming Eq. (20).

The moving heat source is represented mathematically by (Ozisik 1993)

$$g(x,t) = g_0\delta(x - \mathrm{v}t) \tag{4}$$

Where g_o is the heat source intensity and δ is the delta function.The beam is assumed to have the following thermal initial and boundary conditions

$$T(x,0) = T_\infty, \qquad \frac{\partial T}{\partial t}(x,0) = 0, \frac{\partial T}{\partial x}(0,t) = \frac{\partial T}{\partial x}(L,t) = 0 \tag{5}$$

In order to simplify the forms of the equations and use simple numbers in the substitutions, the following dimensionless parameters are introduced

$$\theta = \frac{T-T_\infty}{T_\infty},\ \eta = \frac{t}{t_o},\ \zeta = \frac{x}{\sqrt{\kappa t_o}}, \zeta_o = \frac{L}{\sqrt{\kappa t_o}}, V = \frac{\mathrm{v}}{\sqrt{\kappa/t_o}} \tag{6}$$

Where θ is the dimensionless temperature, η is the dimensionless time, ζ is the dimensionless axial distance, V is the dimensionless heat source speed, and t_o is the reference time, given by: $t_o=(H/2)^2/k$, where k is the thermal diffusivity. Using the above parameters, Eq. (3) becomes

$$\frac{\partial^2\theta}{\partial\zeta^2} - \frac{\partial\theta}{\partial\eta} - \beta\theta = -\gamma\delta\left(\eta - \frac{\zeta}{V}\right) \tag{7}$$

The dimensionless initial and boundary conditions, Eq. (5), become

$$\theta(\zeta,0) = 0, \frac{\partial\theta}{\partial\eta}(\zeta,0) = 0, \frac{\partial\theta}{\partial\zeta}(0,\eta) = \frac{\partial\theta}{\partial\zeta}(\zeta_o,\eta) = 0 \tag{8}$$

Where

$$\beta = \left(\frac{\mathrm{hpt_o}}{\mathrm{DH}\rho\mathrm{c}}\right), \gamma = \left(\frac{\mathrm{g_o}\sqrt{\mathrm{t_0}}}{\mathrm{VT}_\infty\rho\mathrm{c}\sqrt{\mathrm{k}}}\right) \tag{9}$$

Using the Laplace transformation technique with the notation that Laplace transformation of $\theta(\zeta,\eta)$ is given by $\ell\{\theta(\zeta,\eta)\} = \bar{\theta}(\zeta,s)$, Eqs. (7) and (8) take the form

$$\frac{\partial^2\bar{\theta}(\zeta,\mathrm{s})}{\partial\zeta^2} - \lambda_1^2\bar{\theta}(\zeta,\mathrm{s}) = -\gamma\mathrm{e}^{-(\mathrm{s}/\mathrm{v})\zeta} \tag{10}$$

The thermal boundary conditions take the form

$$\frac{\partial\bar{\theta}(0,\mathrm{s})}{\partial\zeta} = \frac{\partial\bar{\theta}(\zeta_\mathrm{o},\mathrm{s})}{\partial\zeta} = 0 \tag{11}$$

Where $\lambda_1^2 = s + \beta$. Eq. (10) subject to the boundary condition Eq. (11) has the following general solution

$$\bar{\theta}(\zeta,s) = \mathrm{C}_1\mathrm{e}^{\lambda_1\zeta} + \mathrm{C}_2\mathrm{e}^{-\lambda_1\zeta} + \mathrm{C}_3\mathrm{e}^{-(\mathrm{s}/\mathrm{v})\zeta} \tag{12}$$

Where

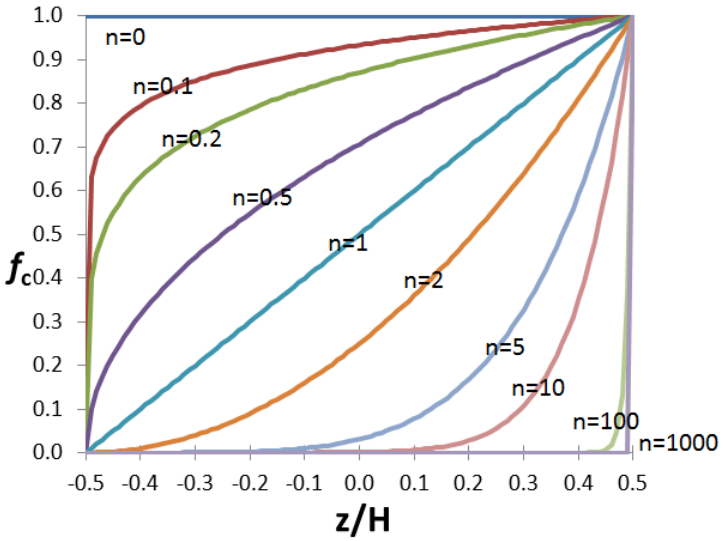

Fig. 2 The effect of the grading parameter *n* on the ceramic volume fraction along the beam

$$C_3 = \frac{\gamma}{\lambda_1^2 - \left({}^{s}/_{V}\right)^2} \tag{13}$$

$$C_2 = \frac{s}{V\lambda_1}\left(\frac{e^{-\left({}^{s}/_{V}\right)\zeta_0} - e^{\lambda_1\zeta_0}}{e^{\lambda_1\zeta_0} - e^{-\lambda_1\zeta_0}}\right)C_3 \tag{14}$$

$$C_1 = C_2 + \left(\frac{s}{V\lambda_1}\right)C_3 \tag{15}$$

In order to describe the composition of the beam shown in Fig. 1, the volume fraction of the ceramic, f_c, and that of metal, f_m are needed. The ceramic volume fraction is given by (Praveen and Reddy 1998)

$$f_c = \left(\frac{z}{H} + \frac{1}{2}\right)^n \quad , \quad -\frac{H}{2} \le z \le \frac{H}{2}, \qquad 0 \le n \le \infty \tag{16}$$

$$f_m = 1 - f_c \tag{17}$$

Where n is the volume fraction exponent, which is a grading parameter that dictates the material variation profile through the thickness of the FGM. Fig. 2 shows the relation between the value of n and the volumetric content of functionally graded material of ceramic and metal, where the lower the value of n means that most of FGM is ceramic and the higher the value indicates the more metal content it has. For n=0, the whole beam is ceramic, while as $n\to\infty$, the whole beam is metal. At the bottom of the beam where (z/H)=-0.5, the material is metal (f_c=0) for all values of n, while at the top of the beam where (z/H)=0.5, the material is ceramic (f_c=1) for all values of n.

In the previous part, the temperature distribution of top layer of the beam was found. This will be used to find the temperature distribution in the next layers in the transverse direction. The need

to find the temperature distribution through the transverse direction of the beam requires finding the thermal gradient along that direction. The governing equation of temperature gradient in the transverse direction is (Prakash *et al*. 2007)

$$\frac{d}{dz}\left[k(z)\frac{dT}{dz}\right] = 0 \tag{18}$$

The thermal boundary conditions are

$$\mathrm{T}(H/2) = \mathrm{T}_c \ \text{and} \mathrm{T}(-\mathrm{H}/2) = \mathrm{T}_m \tag{19}$$

Where T_c is the temperature of the top side of the beam (ceramic), which is the (hot) side. The temperature of the bottom side of the beam (metal) is T_m, which is the (cold) side. The temperature variations that result from this solution can be assumed to take the following exponential form

$$T(z) = ae^{bz} \tag{20}$$

Where a and b are constants that can be found by using curve fit with exponentional charactaristics.The total temperature variations in the beam are found by adding the two temperatures

$$T(x,z,t) = ae^{bz} + T_\infty\theta + T_\infty \tag{21}$$

The mechanical and thermal properties of FGM continuously vary in the transverse direction (i.e., through the thickness). The effective properties of the functionally graded material are obtained by using the power law (Reddy 2004)

$$P(z) = (P_t - P_b)f_c + P_b \tag{22}$$

Where P_t and P_b denote the property of the top layer of the beam (pure ceramic) and bottom layer (pure metal), respectively.

In this work, the FG beam is considered to be temperature dependent where any change in temperature from the reference temperature (300°K) may affect its mechanical and thermal properties. The temperature dependency of the properties takes the following form (Malekzadeh and Beni 2010)

$$P = P_0(P_{-1}T^{-1} + 1 + P_1T^1 + P_2T^2 + P_3T^3) \tag{23}$$

Where P_0, P_{-1}, P_1, P_2 and P_3 represent the temperature-dependent coefficients, such as the elastic modulus E, Poisson's ratio v, mass density ρ and thermal expansion coefficient α.

2.2 Thermoelastic analysis of the FG beam

The beam deflections under consideration are the transverse displacement, $w(x,t)$, and the axial displacement, $u(x,z,t)$, given by

$$u = u_o - z\frac{dw}{dx} \tag{24}$$

Where u_o is the mid-plane deflection. The strain-displacement relation is

$$\varepsilon_{xx} = \frac{du_o}{dx} - z\frac{d^2w}{dx^2} = \varepsilon_{xo} + z\varphi \tag{25}$$

The resulting axial stress takes the form

$$\sigma_{xx} = E\varepsilon_x - \mathrm{E}\alpha T(x,z,t) = E\varepsilon_{xo} + zE\varphi - \mathrm{E}\alpha T(x,z,t) \tag{26}$$

The axial force and bending moment resultants, N and M, are defined by

$$(N,M) = \int_{-H/2}^{H/2} \sigma_{xx}(1,z)dz \tag{27}$$

Substituting and integrating produces the following result

$$\begin{Bmatrix} N \\ M \end{Bmatrix} = \begin{bmatrix} A_{11} & B_{11} \\ B_{11} & D_{11} \end{bmatrix} \begin{Bmatrix} \varepsilon_{x0} \\ \varphi \end{Bmatrix} - \begin{Bmatrix} N^T \\ M^T \end{Bmatrix} \tag{28}$$

Where the beam stiffness coefficients A_{11}, B_{11} and D_{11} are given by the well-known general relation

$$\left(A_{ij}, B_{ij}, D_{ij}\right) = \int_{-\frac{H}{2}}^{\frac{H}{2}} Q_{ij}(z)(1,z,z^2)dz \qquad (i,j = 1,2,6) \tag{29}$$

In the present analysis, the remaining non-zero stiffness constants are given by

$$Q_{11} = \frac{E(z,T)}{1-\nu^2}, \quad Q_{12} = \frac{\nu E(z,T)}{1-\nu^2} \tag{30}$$

Solving for A_{11}, B_{11} and D_{11}

$$A_{11} = \frac{(E_c - E_m)}{(1-\nu^2)} \tag{31}$$

$$B_{11} = \frac{(HE_c - A_{11})}{(1-\nu^2)} \tag{32}$$

$$D_{11} = \frac{(H^2E_c - B_{11})}{(1-\nu^2)} \tag{33}$$

In the present work, only thermal loads are considered, so N and M are zero. The thermal force and the thermal moment are defined by

$$(N^T, M^T) = \int_{-H/2}^{H/2} (1,z)\{Q_{11} + Q_{12}\}\alpha T dz \tag{34}$$

And the strains are

$$\begin{Bmatrix} \varepsilon_{x0} \\ \varphi \end{Bmatrix} = \begin{bmatrix} A_{11} & B_{11} \\ B_{11} & D_{11} \end{bmatrix}^{-1} \begin{Bmatrix} N^T \\ M^T \end{Bmatrix} \tag{35}$$

Which can be written in terms of temperature as

$$\begin{Bmatrix} \varepsilon_{xo} \\ \varphi \end{Bmatrix} = \begin{Bmatrix} I_o + I\theta \\ J_o + J\theta \end{Bmatrix} \tag{36}$$

Where I_o, I, J_o, J are used for abbreviation purposes only. For the beam under consideration, the

following boundary conditions apply

$$w(0,t) = w(L,t) = 0 \tag{37}$$

The value of transverse deflection can be found by solving the following deferential equation

$$\frac{d^2w}{dx^2} = -(J_o + J\theta) \tag{38}$$

A dimensionless transverse deflection is defined as

$$W(\zeta,\eta) = \frac{w(x,t)}{\sqrt{\kappa t_o}} \tag{39}$$

And Eq. (38) becomes

$$\frac{d^2W(\zeta,\eta)}{d\zeta^2} = -\left(\sqrt{\kappa t_o}\right)\left(J_o + J\theta(\zeta,\eta)\right) \tag{40}$$

With the boundary conditions

$$W(0,\eta) = W(\zeta_o,\eta) = 0 \tag{41}$$

Laplace transform of Eqs. (40) and (41)

$$\frac{d^2\bar{W}(\zeta,s)}{d\zeta^2} = -\left(\sqrt{\kappa t_o}\right)\left[\frac{J_o}{s} + J\theta(\zeta,s)\right] \tag{42}$$

$$\bar{W}(0,s) = \bar{W}(\zeta_o,s) = 0 \tag{43}$$

The solution is

$$\bar{W}(\zeta,s) = -\left(\sqrt{\kappa t_o}\right)\left[\frac{J_o\zeta^2}{2s} + J\left(C_1\frac{e^{\lambda_1\zeta}}{{\lambda_1}^2} + C_2\frac{e^{-\lambda_1\zeta}}{{\lambda_1}^2} + C_3V\frac{e^{-(s/V)\zeta}}{s^2}\right) + C_4\zeta + C_5\right] \tag{44}$$

The constants C_1, C_2 and C_3 are already defined in Eqs. (13)-(15). The remaining constants C_4 and C_5 are

$$C_5 = -J\left(\sqrt{\kappa t_o}\right)\left(\frac{C_1}{{\lambda_1}^2} + \frac{C_2}{{\lambda_1}^2} + \frac{C_3V}{s^2}\right) \tag{45}$$

$$C_4 = \left[\frac{J_o\zeta_o^2}{2s} + J\left(C_1\frac{e^{(\lambda_1\zeta_o)}}{{\lambda_1}^2} + C_2\frac{e^{(-\lambda_1\zeta_o)}}{{\lambda_1}^2} + C_3V\frac{e^{-(s/V)\zeta_o}}{s^2}\right) - C_5\right]/\zeta_o \tag{46}$$

The axial deflection is expressed by Eq. (24). Since the value of $w(x, t)$ was found above, the value of the first derivative is easy to be found. The value of u_o can be found by solving the following equation

$$\frac{du_o}{dx} = \varepsilon_{xo} \tag{47}$$

With boundary condition

$$u_o(0,t) = 0 \tag{48}$$

From Eq. (36)

$$\frac{du_o(\mathrm{x,t})}{dx} = I_o + I\theta(\mathrm{x,t}) \tag{49}$$

The dimensionless form of *u* is

$$\mathrm{U_o}(\zeta,\eta) = \frac{\mathrm{u_o(x,t)}}{\sqrt{\kappa \mathrm{t_o}}} \tag{50}$$

The boundary condition becomes

$$U_o(0,\eta) = 0 \tag{51}$$

Eq. (49) becomes

$$\frac{dU_o(\zeta,\eta)}{d\zeta} = I_o + I\theta(\zeta,\eta) \tag{52}$$

By taking Laplace transform of Eq. (52)

$$\frac{d\bar{U}_o(\zeta,s)}{d\zeta} = \frac{I_o}{s} + I\bar{\theta}(\zeta,s) \tag{53}$$

The solution of Eq. (53) is

$$\bar{U}_o(\zeta,s) = \left(\frac{I_o\zeta}{s}\right) + I\left[\frac{C_1}{\lambda_1}e^{\lambda_1\zeta} - \frac{C_2}{\lambda_1}e^{-\lambda_1\zeta} - \frac{C_3V}{s}e^{-(\mathrm{s/v})\zeta}\right] + C_6 \tag{54}$$

Where C_6 is

$$C_6 = I\left[\frac{C_1}{\lambda_1} - \frac{C_2}{\lambda_1} - \frac{C_3V}{s}\right] \tag{55}$$

The value of $\bar{W}(\zeta,s)$ was already found in Eq. (44), so the first derivative is equal

$$\frac{\mathrm{d}\bar{W}(\zeta,\mathrm{s})}{\mathrm{d}\zeta} = -\left(\sqrt{\kappa \mathrm{t_o}}\right)\left[\frac{J_o\zeta}{\mathrm{s}} + \mathrm{J}\left(\mathrm{C_1}\frac{\mathrm{e}^{\lambda_1\zeta}}{\lambda_1} - \mathrm{C_2}\frac{\mathrm{e}^{-\lambda_1\zeta}}{\lambda_1} - \mathrm{C_3V}\frac{\mathrm{e}^{-(\mathrm{s/v})\zeta}}{S}\right) + \mathrm{C_4}\right] \tag{56}$$

3. Solution

In order to determine the temperatures and deflections of the FG beam, Eqs. (12), (44) and (54) are inverted into time domain using the Riemann-sum approximation method. In this method, any function $\bar{f}(\zeta,s)$ is inverted into the time domain as (Tzou 1997)

$$f(\zeta,\eta) = \frac{e^{\varepsilon\eta}}{\eta}\left(\frac{1}{2}\bar{f}(\zeta,\psi) + \mathrm{Re}\sum_{n=1}^{N}\bar{f}(\zeta,\psi+\frac{in\pi}{\eta})(-1)^n\right) \tag{57}$$

Where *Re* is the (real part of) and *i* is the complex number $\sqrt{-1}$. In Eq. (57) $f(\zeta, \eta)$, represents either θ, *W* or *U*. For faster convergence, numerous numerical experiments have shown that the value of Ψ satisfying the relation ($\Psi\eta \approx 4.7$) gives the most satisfactory results.

Table 1 Temperature-dependent coefficients of ceramic (Si3N4) and metal (SUS304)

FGM component	Property	P_{-1}	P_o	P_1	P_2	P_3
Ceramic (Si3N4)	E (N/m)	0	348.43×10^{9}	-3.07×10^{-4}	2.16×10^{-7}	-8.946×10^{-11}
	V	0	0.24	0	0	0
	α (1/K)	0	5.87×10^{-6}	-9.095×10^{-4}	0	0
	ρ (kg/m^3)	0	2370	0	0	0
	k (W/m.K)	0	9.19	0	0	0
Metal (SUS304)	E (N/m)	0	201.04×10^{9}	3.079×10^{-4}	-6.534×10^{-7}	0
	V	0	0.3262	-2.002×10^{-4}	3.797×10^{-7}	0
	α (1/K)	0	12.33×10^{-6}	8.086×10^{-4}	0	0
	ρ (kg/m^3)	0	8166	0	0	0
	k (W/m.K)	0	12.04	0	0	0

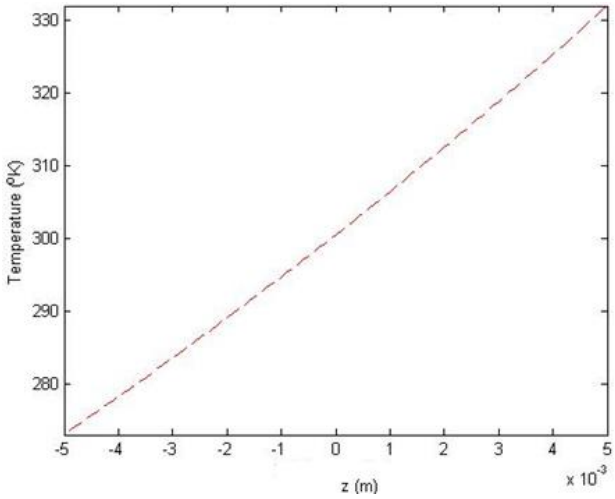

Fig. 1 Temperature distribution as a function of the transverse direction (z)

4. Results and discussion

In this study the values of the parameters used are as follows (unless otherwise stated, i.e., when the effect of a certain parameter is investigated): beam dimensions H=0.01 m, D=0.01 m, L=0.5 m. The heat source intensity $g_o=1\times10^5$W/m^3 and the heat source speed $v=5\times10^{-3}$ m/s. The ambient temperature T_∞ is 273^{o}K and the heat convection coefficient h is 20 W/m^2.K. The FGM used in the analysis is Si3N4 ceramic SUS304 metal alloy. Both parts of the functionally graded material are considered temperature dependent (Eq. (23)) with the properties given in Table 1.

4.1 Temperature distribution

Finding the temperature distribution throughout the FGM beam is the main step in this work as it provides the thermal behavior of the beam as a result of the motion of the heat source. The

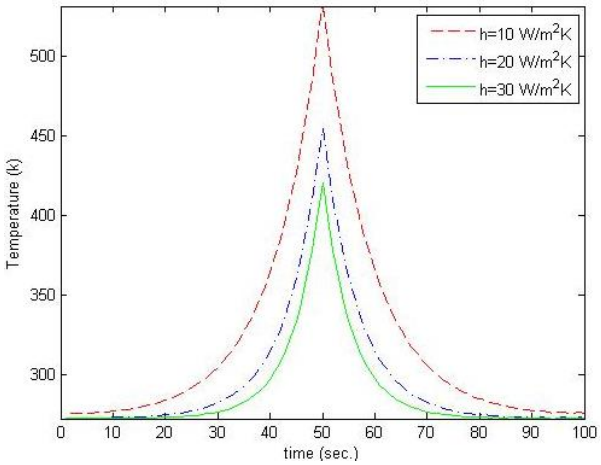

Fig. 4 Variation of beam mid-point temperature with time for different values of the heat convection coefficient

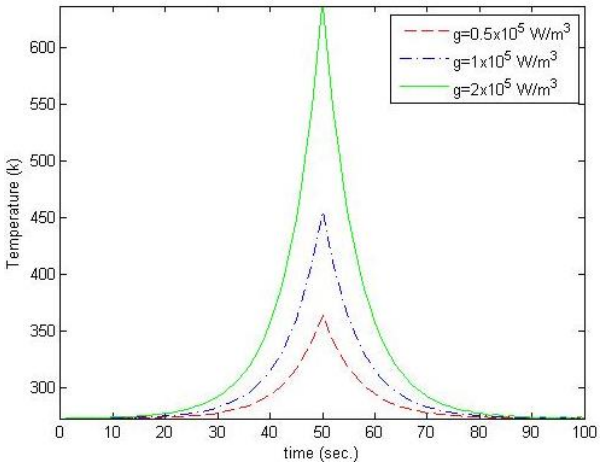

Fig. 5 Variation of beam mid-point temperature with time for different values of the heat source intensity

temperature variations as function of the transverse direction are shown in Fig. 3. As shown in the figure, the temeprature has its maximum value at the top surface of the beam (ceramic), which is the (hot) side where the heat source is acting directly. The heat source is only applied for a short time, so the temperature at the bottom of the beam (metal) is still equal to the ambient temperature (the cold side). By curve fitting of the data in the figure, the values of the constants in Eq. (20) are found and the equation takes the following form

$$T(z) = 300.7e^{19.5z} \tag{58}$$

This equation is considered as a material charactaristic curve where it won't be different if the heat source velocity or intensity are changed.This temperature is added to the temperature variation, as shown by Eq. (21), in order to determine the transient temperature distribution of the beam.

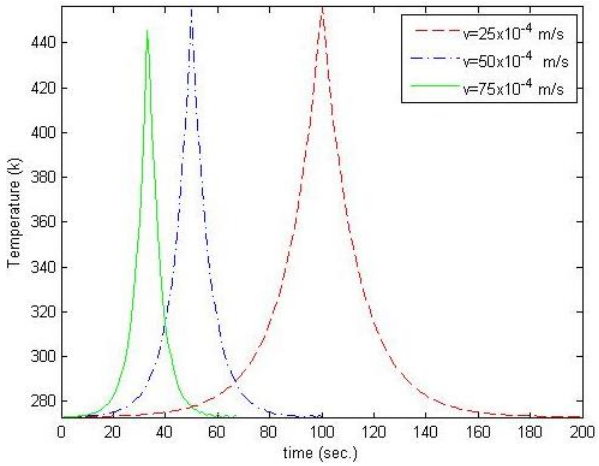

Fig. 6 Variation of beam mid-point temperature with time for different values of the heat source velocity

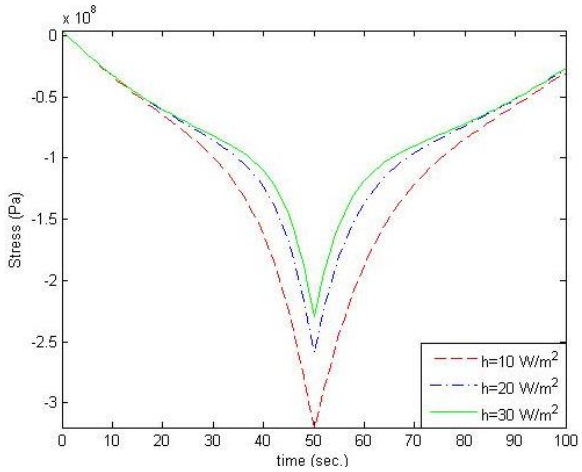

Fig. 7 Variation of stress at the beam mid-point with time for different values of the heat convection coefficient

Fig. 4 shows the variation of the temperature of the midpoint of the beam with time for different values of the heat convection coefficient. It can be seen that the temperature increases with time and reaches its maximum value at time t=50 seconds (which is the time at which the heat source passes the midpoint of the beam), and then decreases. The effect of heat convective losses on the beam thermal behavior is clear: as h increases, the thermal losses increase and the beam temperature decreases.

Fig. 5 shows the variation of the temperature with time while the heat source with different intensities travels along the beam. It can be noticed that the beam temperature increases significantly with higher heat source intensity due to the amount of energy added. Fig. 6 shows the effect of heat source velocity on the midpoint temperature of the beam, where the maximum temperature value for each case (peak of the curve) occurs when the heat source passes that point. It is also noticed that the temperature increases with lower heat source speeds since each specified

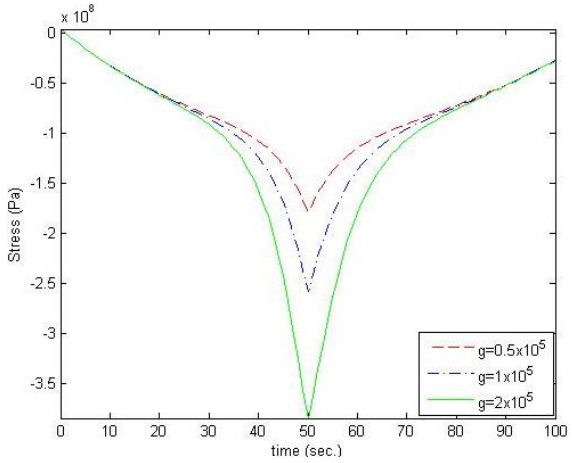

Fig. 8 Variation of stress at the beam mid-point with time for different values of the heat source intensity

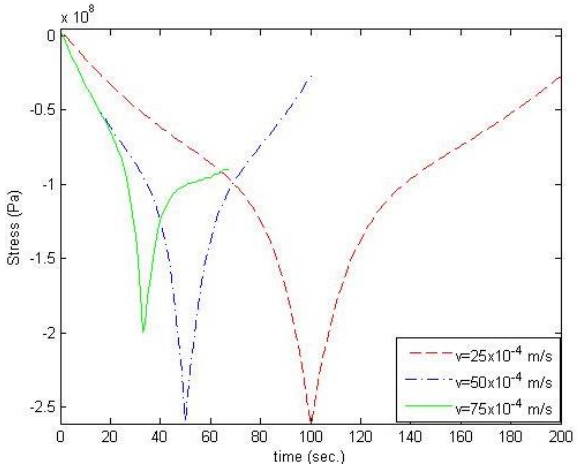

Fig. 9 Variation of stress at the beam mid-point with time for different values of the heat source velocity

location receives more amount of energy as the source speed decreases. This results from the intensity of the released energy that increases as the heat source speed decreases.

4.2 Beam deflections and stresses

Fig. 7 shows the variation of the axial stress at midpoint of the beam with time for different values of heat convection coefficients. Due to the support conditions and the heating process, the stresses are compressive. The behavior in this figure is based on the thermal history which was depicted in Fig. 4. It can be seen that the compressive stress values increase with time and reach the maximum values at t=50 (which is the time at which the heat source passes the midpoint of the beam), and then decrease. It can also be seen that for higher values of the heat convection coefficient, the thermal losses increase and the beam temperature decreases and results in lower values of stress.

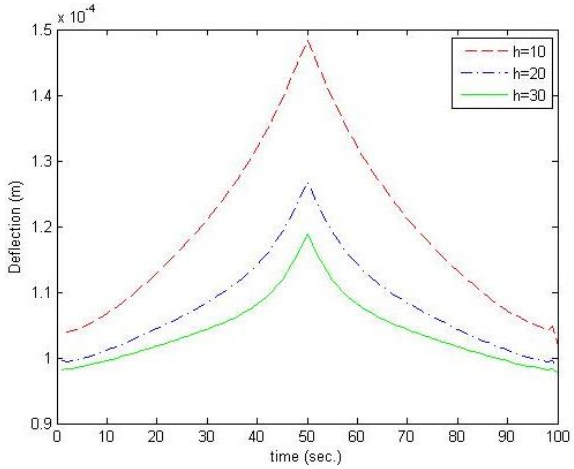

Fig. 10 Variation of the transverse deflection of the beam mid-point with time for different values of the heat convection coefficient

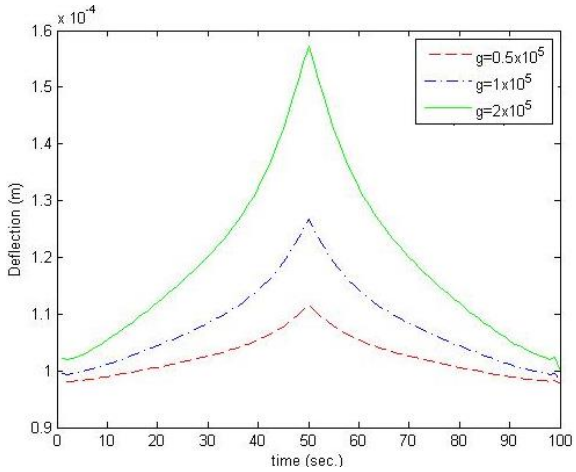

Fig. 11 Variation of the transverse deflection of the beam mid-point with time for different values of the heat source intensity

Figs. 8 and 9 present the effects of the heat source intensity and speed, respectively, on the axial stress of the midpoint of the beam. Based on the discussions of Figs. 5 and 6, the behavior off the stress is easily explained where it is clear that compressive stresses increase with higher heat source intensity and lower speeds.

Figs. 10, 11, and 12 present the effects of the heat convection coefficient, the heat source intensity and the heat source speed, respectively, on the transverse deflection of the midpoint of the beam. Based on the discussions of Figs. 4, 5 and 6, the behavior of the deflection is easily explained where it is clear that the deflections increase with lower convection coefficients, higher heat source intensities and lower speeds.

The FGM properties throughout this work were considered to be temperature dependent for the accuracy of the results. In Fig. 13, a comparison is presented between a case with temperature-dependent and a case with temperature-independent material properties on the transverse

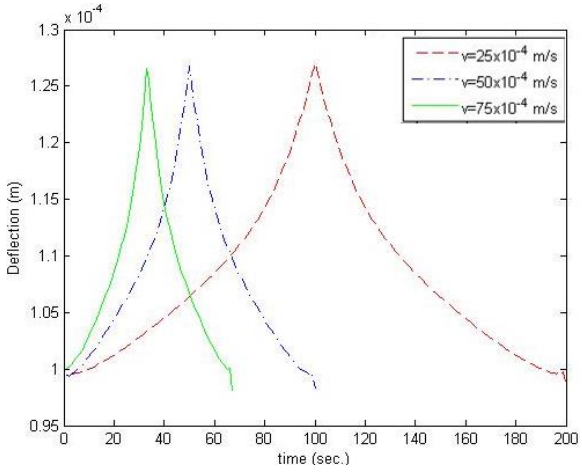

Fig. 12 Variation of the transverse deflection of the beam mid-point with time for different values of the heat source velocity

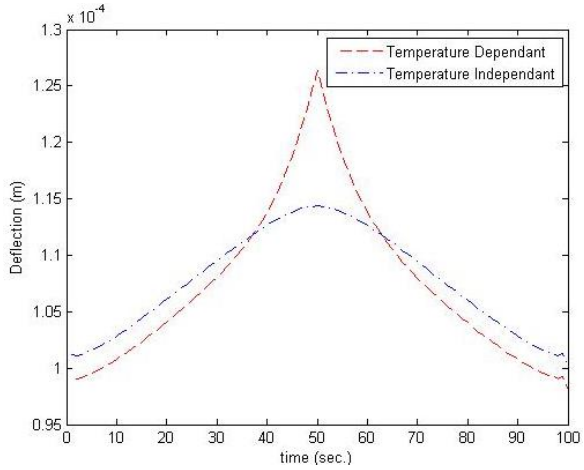

Fig. 13 The transverse deflection beam midpoint for temperature dependent and temperature independent FGM properties

deflection of the beam midpoint. The figure shows an important fact that neglecting the temperature-dependency of the properties results in less accurate results. The more important point here is the underestimation of the value of the maximum deflection.

5. Conclusions

The thermo-mechanical behavior of a simply supported functionally graded material beam under the effect of a moving heat source is investigated. The transient temperatures, deflections and stresses are calculated and presented for some specific cases. The FGM consists of a metal part (bottom) and ceramic part (top) where grading is in the transverse direction, with the properties being temperature-dependent. All material properties are calculated by using the power

law. The material properties in the axial direction are the same. The heat source motion takes place along the beam on the top surface where the material is ceramic (the hot side), while the bottom surface where the material is metallic is the cold side.

The temperature distribution is found by superposition of the temperature variation through the transverse direction, within the FGM, and the variation in the axial direction, resulting from the motion of the heat source. Based on the temperature history within the beam, the thermally-induced deflections and stresses are found.

The thermos-elastic modeling approach consisted of formulating the partial differential equations for the temperatures and deflections in time and space, then using Laplace transformation to transform them into ordinary differential equations, and finally using the inverse Laplace transformation to find the solutions.

The temperature, deflection and stress time histories of the beam are presented. The effects of different parameters, such as the convection coefficient and the heat source intensity and speed are investigated. The results show that temperatures, and hence the deflections and stresses increase with less heat convection from the beam surface, higher heat source intensity and low speeds.

References

Akbaş, S.D. (2015), "Wave propagation of a functionally graded beam in thermal environments", *Steel Compos. Struct.*, **19**(6), 1421-1447.

Al-Huniti, N.S. (2004), "Dynamic behavior of a laminated beam under the effect of a moving heat source", J. *Compos. Mater.*, **38**(23), 2143-2160.

Al-Huniti, N.S., Al-Nimr, M.A. and Daas, M.A. (2004), "Transient variations of thermal stresses and the resulting residual stresses within a thin plate during welding processes", *J. Therm. Stress.*, **27**(8), 671-689.

Al-Huniti, N.S., Al-Nimr, M.A. and Naij, N. (2001), "Dynamic response of a rod due to a moving heat source under the hyperbolic heat conduction model", *J. Sound Vibr.*, **242**(4), 629-640.

Daouadji, T.H. and Adim, B. (2016), "Theoretical analysis of composite beams under uniformly distributed load", *Adv. Mater. Res.*, **5**(1), 1-9.

Ding, H., Huang, D. and Chen, W. (2007), "Elasticity solutions for plane anisotropic functionally graded beams", *J. Sol. Struct.*, **44**(1), 176-196.

Ebrahimi, F., Ehyaei, J. and Babaei, R. (2016), "Thermal buckling of FGM nanoplates subjected to linear and nonlinear varying loads on Pasternak foundation", *Adv. Mater. Res.*, **5**(4), 245-261.

Freund, L.B. (1993), "Stress distribution and curvature of a general compositionally graded semiconductor layer", *J. Cryst. Grow.*, **132**(1-2), 341-344.

Jiang, A. and Ding, H. (2005), "The analytical solutions for orthotropic cantilever beams (I) subjected to surface forces", *J. Zhejiang Univ.*, **6**(2), 126-131.

Jooybar, N., Malekzadeh, P. and Fiouz, A. (2016a), "Vibration of functionally graded carbon nanotubes reinforced composite truncated conical panels with elastically restrained against rotation edges in thermal environment", *Compos. Part B: Eng.*, **106**(1), 242-261.

Jooybar, N., Malekzadeh, P., Fiouz, A. and Vaghefi, M. (2016b), "Thermal effect on free vibration of functionally graded truncated conical shell panels", *Thin-Wall. Struct.*, **103**, 45-61.

Kadoli, R., Akhtar, K. and Ganesan, N. (2008), "Static analysis of functionally graded beams using higher order shear deformation theory", *Appl. Math. Model.*, **32**(12), 2509-2525.

Koizumi, M. (1997), "FGM Activities in Japan", *Compos. Part B*, **28**(1-2), 1-4.

Lee, P.H. (2013), "Fabrication, characterization and modeling of functionally graded materials", Ph.D. Dissertation, Columbia University, New York, U.S.A.

Malekzadeh, P. and Alibeygi, B.A. (2010), "Free vibration of functionally graded arbitrary straight-sided quadrilateral plates in thermal environment", *Compos. Struct.*, **92**(11), 2758-2767.

Malekzadeh, P. and Heydarpour, Y. (2012), "Free vibration analysis of rotating functionally graded cylindrical shells in thermal environment", *Compos. Struct.*, **94**(9), 2971-2978.
Malekzadeh, P. and Heydarpour, Y. (2012), "Response of functionally graded cylindrical shells under moving thermo-mechanical loads", *Thin-Wall. Struct.*, **58**, 51-66.
Malekzadeh, P. and Monajjemzadeh, S.M. (2016), "Dynamic response of functionally graded beams in a thermal environment under a moving load", *Mech. Adv. Mater. Struct.*, **23**(3), 248-258.
Malekzadeh, P. and Shojaee, A. (2014), "Dynamic response of functionally graded beams under moving heat source", *J. Vibr. Contr.*, **20**(6), 803-814.
Malekzadeh, P. and Shojaee, S.A. (2013), "Dynamic response of functionally graded plates under moving heat source", *Compos. Part B: Eng.*, **44**(1), 295-303.
Nakamura, T., Wang, T. and Sampath, S. (2000), "Determination of properties of graded materials by inverse analysis and instrumented indentation", *Acta Mater.*, **48**(17), 4293-4306.
Ozisik, M.N. (1993), *Heat Conduction*, Wiley, New York, U.S.A.
Prakash, T. Singha, M. and Ganapathi, M. (2007), "Thermal post buckling analysis of FGM skew plates", *Eng. Struct.*, **30**(1), 22-32.
Praveen, G.N. and Reddy, J.N. (1998), "Nonlinear transient thermoelastic analysis of functionally graded ceramic-metal plates", *J. Sol. Struct.*, **35**(33), 4457-4476.
Reddy, J.N. (2004), *Mechanics of Laminated Composite Plates and Shells: Theory and Analysis*", CRC Press, Boca Raton, FL.
Sankar, B. (2001), "An elasticity solution for functionally graded beams", *Compos. Sci. Technol.*, **61**(2), 689-696.
Sankar, B. and Tzeng, T. (2002), "Thermal stresses in functionally graded beams", *AIAA J.*, **40**(6), 1228-1232.
Simsek, M. (2010), "Vibration analysis of a functionally graded beam under a moving mass by using different beam theories", *Compos. Struct.*, **92**(4), 904-917.
Tzou, D. (1997), *Macro-to-Microscale Heat Transfer*, Taylor and Francis, Washington, U.S.A.
Wang, R. and Pan, E. (2011), "Three dimensional modeling of functionally graded multiferroic composites", *Mech. Adv. Mater. Struct.*, **18**(1), 68-76.
Zamanzadeh, M., Rezazadeh, G., Ilgar, J. and Shabani, R. (2014), "Thermally induced vibration of a functionally graded micro-beam subjected to a moving laser beam", *J. Appl. Mech.*, **6**(6), 1450066.
Zenkour, A.M. and Abouelregal, A.E. (2014), "Vibration of FG nanobeams induced by sinusoidal pulse-heating via a nonlocal thermoelastic model", *Acta Mech.*, **225**(12), 3409-3421.
Zhu, H. and Sankar, B. (2004), "A combined fourier series-Galerkin method for the analysis of functionally graded beams", *J. Appl. Mech.*, **71**(3), 421-424.

OP